Robust Control of Electrified Turbocharged Diesel Engines

Dezong Zhao, *Member, IEEE*, Edward Winward, Zhijia Yang, Richard Stobart, *Member, IEEE*, and Thomas Steffen

***Abstract*— Electrified turbocharger is a critical technology for engine downsizing and is a cost-effective solution for exhaust gas energy recovery. In conventional turbocharged diesel engines, the air path holds strong nonlinearity since the actuators are all driven by the exhaust gas. In an electrified turbocharged diesel engine (ETDE), the coupling is more complex, due to the electric machine mounted on the turbine shaft impacts the exhaust manifold dynamics as well. In distributed single-input single-output control methods, the gains tuning is time consuming and the couplings are ignored. To control the performance variables independently, developing a promising multi-input multi-output control method for the ETDE is essential. In this paper, a model-based multi variable robust controller is designed to control the performance variables in a systematic way. Both simulation and experimental results verified the effectiveness of the proposed controller.**

I. Introduction

In the Paris Climate Change Conference 2015, countries of the world have made an agreement that to limit the global average temperature increase below 2 °C, with an aspiration of below 1.5 °C above the pre-industrial level [1]. Hard efforts need to do to reduce greenhouse gas (GHG) emissions effectively in the following decades. Transportation sector accounts for about a quarter of GHG emissions and a half of global oil consumption, which is the the second largest source of GHG emissions [2]. The fuel consumption reduction in transportation sector is a global critical issue.

Engine downsizing is proven as the most promising approach in fuel consumption reduction [3]–[5], which uses a smaller capacity engine to provide the power of a larger engine. The downsized engine allows a larger area of its operating range to be more efficiently used for most of the time, since the average engine operating points become closer to its high fuel efficiency zone. At high loads, the loss of reduced engine displacement is compensated by effective air charging. Variable geometry turbocharger (VGT) is an effective turbocharging technology, which has been widely used in modern diesel engines. The VGT can provide power to drive the compressor running at different desired boost levels by tuning the effective nozzle area. In VGT-equipped engines , for part of the exhaust gas energy is used to accelerate the turbine shaft speed for boosting, both engine transient response and fuel economy are improved. However, the turbo-lag in the VGT is still non-negligible. To overcome the transient performance limitations, a fast boosting system is required to work cooperating with the VGT [6], which is the motivation for the electrification of turbo-machinery [7]. The electrified turbocharger is the cutting edge e-boosting system for its high efficiency.

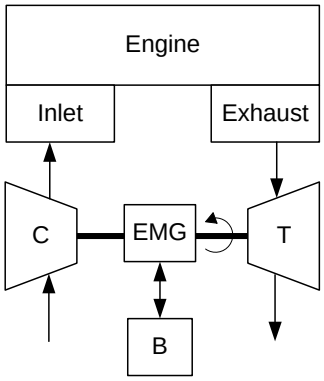

Fig. 1. Electrified turbocharger, C: compressor; T: turbine; B: battery; EMG: electric motor/generator

The electrified turbocharger has an electric motor/generator (EMG) mounted on the turbine shaft, as shown in Fig. 1. At low engine speeds, the energy is used to assist the turbine shaft. In this case the electrified turbocharger works as a power assist system and therefore, the turbo-lag is greatly minimized. At engine high power regions, the energy is extracted from the turbine shaft to the energy storage, which indicates part of the exhaust gas energy is recovered. The energy storage is placed as a buffer that either supplies energy to assist the compressor or absorbs energy from the exhaust gas. Compared with the electric turbocompounding, the electrified turbocharger has less pumping losses in the initial phase and less mechanical losses. Therefore, the electrified turbocharger is seen as the prime candidate for the electrification of turbo-machinery. The mainstream diesel engine and turbocharger manufacturers have developed [8]–[10] or are developing their own prototype electrified turbochargers [11], as shown in Fig. 2.

Developing effective control methods for electrified turbochargers is critical to explore the maximum potential of downsized engines. Although some efficiency mapping work have been done in experiments [12]–[16], a proper control solution is still lacking. A multi-variable control framework of an electrified turbocharged diesel engine (ETDE) is proposed in this paper, and it is successfully validated on a state-of-the-art electrified engine test chassis.

D. Zhao, Z. Yang, R. Stobart, and T. Steffen are with Department of Aeronautical and Automotive Engineering, Loughborough University, Loughborough, Leicester, UK (e-mail: d.zhao2@lboro.ac.uk, z.yang2@lboro.ac.uk, r.k.stobart@lboro.ac.uk, t.steffen@lboro.ac.uk).

E. Winward is with Energy and Transportation Research, Caterpillar Inc., Peterborough, UK.

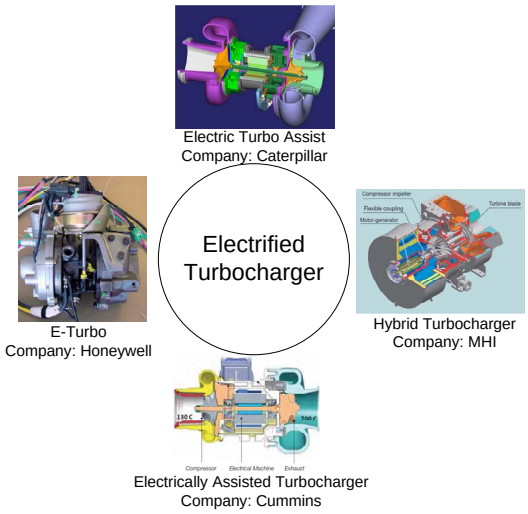

Fig. 2. Family of electrified turbochargers

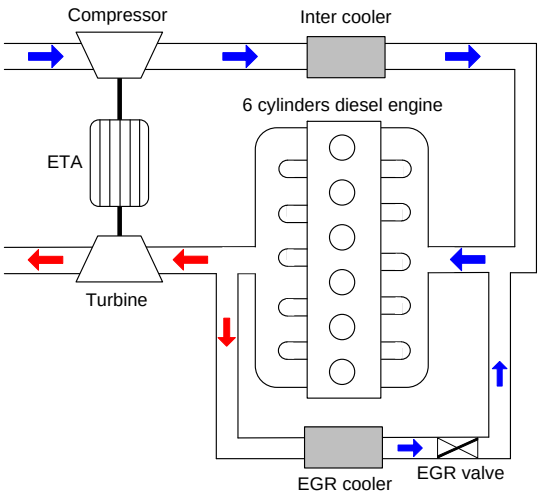

Fig. 3. Electrified turbocharged diesel engine

The paper is organized as follows. After the introduction in section I, the ETDE model is described in section II. The controller design is presented in section III. Experimental validation results are demonstrated in section IV. Finally, the conclusions are summarized in section V.

II. System Description and Characterization

The layout of the ETDE is illustrated as Fig. 3, while the essential variables is listed in Table I. The electrified turbocharger is composed of a compressor, a turbine, and an EM on the turbine shaft. The turbine takes exhaust gas energy to power the compressor for fresh air delivery. The EGR loop feeds back part of exhaust gas to the intake manifold, to lower the combustion temperature for NO_x reduction. The control-oriented mean value model of a turbocharged diesel engine can be found in [17]. The EM can be used to accelerate or decelerate the turbine speed, so it is also called the electric turbo assist (ETA). A switched reluctance motor (SRM) is selected as the EM for it is an excellent option in extra-high speed applications thanks to its simple structure. The simple SRM structure results in a high rotor temperature capability and no concern about the high cost of rare-earth materials. The ETA can work in both assisting (motoring) mode and harvesting (generating) mode. In assisting mode, the ETA extracts energy from the battery to assist boosting. In harvesting mode, the additional turbine torque resulting from exceed exhaust energy causes a power flow to the battery.

TABLE I
Nomenclature

Variable	Description	Unit
N	Engine speed	rpm
T_L	Engine load	Nm
W_f	Engine fuelling rate	kg/s
W_c	Compressor air mass flow rate	kg/s
W_{egr}	EGR mass flow rate	kg/s
W_t	Turbine gas mass flow rate	kg/s
P_c	Compressor power	kW
P_t	Turbine power	kW
P_{em}	EM power	kW
P_{bl}	Power to overcome bearing losses	kW
P_{wl}	Power to overcome windage losses	kW
p_{in}	Intake manifold pressure	kPa
p_{exh}	Exhaust manifold pressure	kPa
p_{am}	Ambient pressure	kPa
T_{am}	Ambient temperature	K
ω	Turbine speed	rpm
τ	Turbocharger time constant	s
η_c	Compressor isentropic efficiency	–
η_t	Turbine isentropic efficiency	–
η_m	Turbocharger mechanical efficiency	–
χ_{egr}	EGR valve position	–
χ_{vgt}	VGT vane position	–
c_p	Specific heat at constant pressure, 1.01	kJ/(kgK)
c_v	Specific heat at constant volume, 0.718	kJ/(kgK)
μ	$1 - c_v/c_p$	–

The dynamics of the turbocharger can be modeled as a first-order lag power transfer function with time constant τ:

$$\dot{P}_c = \frac{1}{\tau}\left(P_t + P_{em} - P_{bl} - P_{wl} - P_c\right). \tag{1}$$

Using the mechanical efficiency to represent energy losses, (1) can be represented as

$$\dot{P}_c = \frac{1}{\tau}\left(\eta_m\left(P_t + P_{em}\right) - P_c\right). \tag{2}$$

W_c is related to P_c by

$$W_c = \frac{\eta_c}{c_p T_{am}} \frac{P_c}{\left(\frac{p_{in}}{p_{am}}\right)^{\mu} - 1}, \tag{3}$$

and P_t can be expressed by W_t:

$$P_t = \eta_t c_p T_{exh}\left(1 - \left(\frac{p_{am}}{p_{exh}}\right)^{\mu}\right) W_t. \tag{4}$$

The key in the control of the diesel engine to follow exhaust emission regulations is keeping fair values of air-fuel ratio and EGR fraction. In the air path variables of the ETDE, p_{in} and p_{exh} determine the amount of gas to boost the compressor for fresh air delivery, and W_{egr} decides

the amount of feedback exhaust gas. Therefore, the control variables are selected as

$$y = \left[p_{in}, \quad p_{exh}, \quad W_{egr}\right]^{\mathrm{T}}, \tag{5}$$

with the control inputs of

$$u = \left[\chi_{vgt}, \quad P_{em}, \quad \chi_{egr}\right]^{\mathrm{T}}. \tag{6}$$

By regulating each element in y independently, the desired air path dynamics of the ETDE is expected to achieved in both transients and steady states.

III. Robust Controller Design

The single-input single-output (SISO) proportional-integral (PI) controllers are widely used in the control of conventional turbocharged diesel engines, while p_{in} and W_{egr} are controlled by χ_{vgt} and χ_{egr}, respectively. The gain values of PI controllers are generally tuned in off-line calibration. However, in the ETDE, the dynamics have been significantly changed, therefore the controllers require to be re-designed, which is a time-consuming work. Considering strong internal interactions among different loops, designing a model-based decoupling multi-input multi-output (MIMO) controller is a feasible approach. The H_∞ control is employed to build the decoupling controller for its advantages over internal couplings.

A. Control Problem Formulation

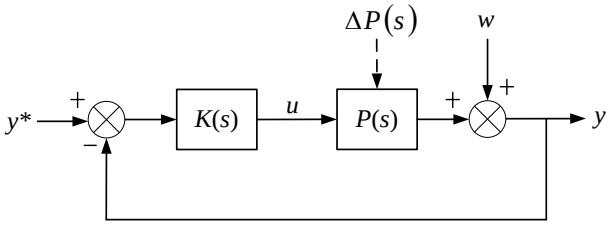

Fig. 4. Closed loop control diagram

A general closed loop control diagram is shown as Fig. 4. It is expected that the system can behave both high performance and high robustness in face of model uncertainty $\Delta P(s)$ and measurement noise w. The transfer function from w to y is denoted as the sensitivity function $S(s)$:

$$S(s) = 1/(1 + K(s)P(s)), \tag{7}$$

with $P(s)$ and $K(s)$ are the trasfer function of plant and controller, respectively. The transfer function from reference y^* to output y is $G(s)$, which can also be denoted as the complementary sensitivity function:

$$T(s) = K(s)P(s)/(1 + K(s)P(s)), \tag{8}$$

while the loop function is defined as

$$L(s) = K(s)P(s). \tag{9}$$

From the physical point of view, reference commands normally consist of low frequency components. In contrast, unmodelled dynamics, model uncertainties, and noises are

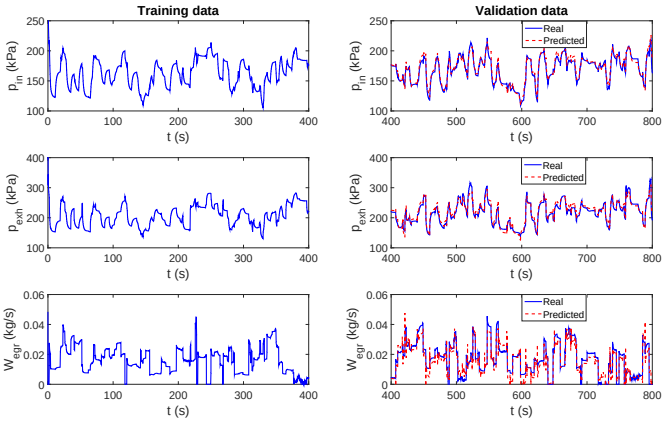

Fig. 5. Training and validation in model identification

mainly composed by high frequency components. To keep the balance between robustness and performance, $S(s)$ should be small at low frequencies for good tracking, and $T(s)$ should be small at high frequencies for good noise rejection [18]. The controller $K(s)$ is to be designed such that:

$$\min_{K(s)} \gamma : \overline{\sigma} \begin{bmatrix} T(s) \\ S(s) \end{bmatrix} < \gamma, \tag{10}$$

where $\overline{\sigma}$ denotes the maximum singular value, and γ is the upper limit. This is to solve a H_∞ problem and very applicable in MIMO systems. Since $S(s) + T(s) = 1$ is held for all frequencies, the control problem is translated to the design of the open-loop transfer function such that $|L(s)| \gg 1$ in low frequencies, and $|L(s)| \ll 1$ in high frequencies. Therefore, the control problem is further transferred to set the proper value on crossover frequency for both strong disturbance attenuation (for tracking) and high robust stability (for noise rejection) [19]. It is expected to design a suitable $L(s)$ with the specified crossover frequency ω_c, and the approach is called H_∞ loop shaping. However, in a MIMO system, the $L(s)$ has multiple trajectories. Therefore, designing a $L(s)$ locating within upper and lower bounds for all frequencies is a more feasible approach.

B. Model Identification

The state space model of the ETDE is to be identified from the time domain data, where the model order and coefficient matrices are both to be determined. As an example, the model identification at the operating point of 1800 rpm and 260 Nm is illustrated in Fig. 5. The calibration has continued for 800 seconds, while the action ranges of χ_{vgt}, P_{em}, and χ_{egr} are limited as [0.2, 0.8], [-1.5 kW, 1.5 kW], and [0, 0.3], respectively. In the model generation and validation, the first half 400 seconds data are used for training and the latter half 400 seconds data are used for validation. By comparing the fitting results, a third-order model with the highest score is selected as the proper model at the specified operating point. The fitting score on p_{in}, p_{exh}, and W_{egr} are 81%, 79%, and 73%, respectively.

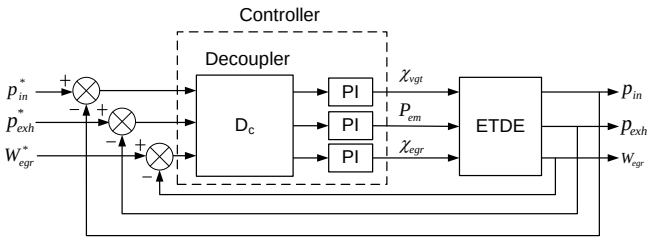

Fig. 6. The diagram of ETDE air path control

C. Controller Synthesis

Based on the identified coefficient matrices, the transfer function of the ETDE model is given as

$$P(s) = C\left(sI - A\right)^{-1} B + D. \tag{11}$$

The control target is to design a $K(s)$ such that $G(s) \simeq 1$ at low frequencies and $G(s) \gg 1$ at high frequencies. In the H_∞ loop shaping controller design, a pre-scaling matrix S_1 and a post-scaling matrix S_2 are applied on $P(s)$ to make sure that each input and output are treated equivalently in the MIMO system:

$$P_s(s) = S_2 P(s) S_1. \tag{12}$$

The singular values of the scaled plant $P_s(s)$ are shaped using a pre-compensator W_1 and a post-compensator W_2 to get the desired loop shape [20], [21]. The weighted plant model is

$$P_w(s) = W_2 P_s(s) W_1. \tag{13}$$

An optimal stabilizing controller K_∞ is to be designed to minimize the singular value such that [22]:

$$\gamma_{\text{opt}} = \min_{K_\infty} \left\| \begin{bmatrix} K_\infty \\ I \end{bmatrix} \left(I - P_w K_\infty\right)^{-1} \begin{bmatrix} P_w I \end{bmatrix} \right\|. \tag{14}$$

The final controller $K(s)$ is constructed by combining K_∞, W_1, W_2, S_1, and S_2:

$$K = W_1 S_1 K_\infty S_2 W_2. \tag{15}$$

The H_∞ loop shaping controller is designed in the form of decoupling PI controllers, as shown in Fig. 6, where p^*_{in}, p^*_{exh}, and W^*_{egr} are the setpoints of p_{in}, p_{exh}, and W_{egr}, respectively. According to engineering experiences, the crossover frequencies of all loops are specified in the band of

$$\omega_c \in \left[1 \text{ rad/s}, \quad 10 \text{ rad/s}\right]. \tag{16}$$

The controller is performed in a Simulink setup via the use of Matlab function *looptune* provided in the Robust Control Toolbox. The Bode diagram of the original ETDE model $P(s)$ and the resulting closed loop transfer function $G(s)$ at 1800 rpm, 260 Nm are shown in Fig. 7. The loop shaping results show that the closed loop response is close to 0 dB/decade at low frequencies and roll off with a high rate at high frequencies, indicating the shaped closed loop control system achieves both strong noise attenuation performance and high stability.

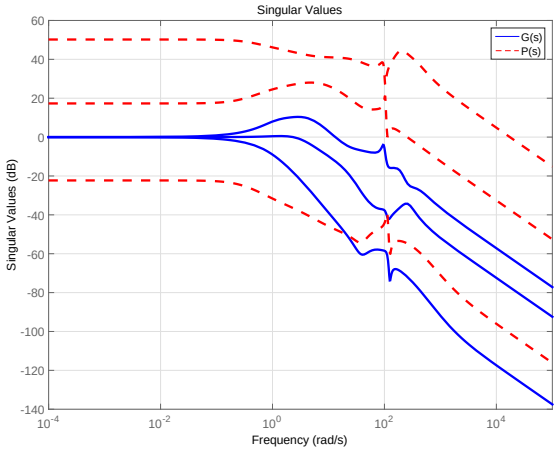

Fig. 7. Singular values of nominal plant and shaped plant

IV. Simulation Results

Prior to the experiments, the controller has been validated on an ETDE mean value model in Simulink, while the model is identified from calibration data on a heavy-duty ETDE in the test cell. The engine operating point is selected as 1800 rpm, 260 Nm, while the engine model at this point has been identified in Section V. Using the Matlab command *looptune*, the decoupling matrix, together with the proportional and integral gains of the PI controllers in the 3 loops are built as following:

$$D_c = \begin{bmatrix} -0.0774 & -0.0606 & -47.46 \\ 0.0757 & -0.0092 & 18.4 \\ 0.4879 & 0.0987 & 602.8 \end{bmatrix},$$
$$K_P = \begin{bmatrix} -0.0007 & 0.0725 & 0.0005 \end{bmatrix}^{\text{T}},$$
$$K_I = \begin{bmatrix} 0.776 & 3.8 & 0.0272 \end{bmatrix}^{\text{T}}.$$

The initial values of the setpoints are chosen as

$$y^* = \begin{bmatrix} 150 \text{ kPa} & 200 \text{ kPa} & 0.02 \text{ kg/s} \end{bmatrix}^{\text{T}}.$$

Step changes on the command signals are made on p^*_{in}, p^*_{exh}, and W^*_{egr} at 10 s, 20 s, and 30 s, respectively. After the step changes, the command values are

$$y^* = \begin{bmatrix} 190 \text{ kPa} & 260 \text{ kPa} & 0.03 \text{ kg/s} \end{bmatrix}^{\text{T}}.$$

The tracking performance is evaluated in Fig. 8. All the performance variables are tracked fast and accurately. When step changes occur on command values, small spikes are observed but the trajectories are attracted to the updated command values quickly. The controller addresses the tracking of multiple variables in a systematic manner. The simulation results validate the effectiveness of the proposed controller, and build the confidence to expand to experimental tests.

V. Experimental Results

The experimental platform is shown as Fig. 9. The investigated engine is a six-cylinder, 7.01-L heavy-duty engine with rated power of 225 kW at 2200 rpm and a rated

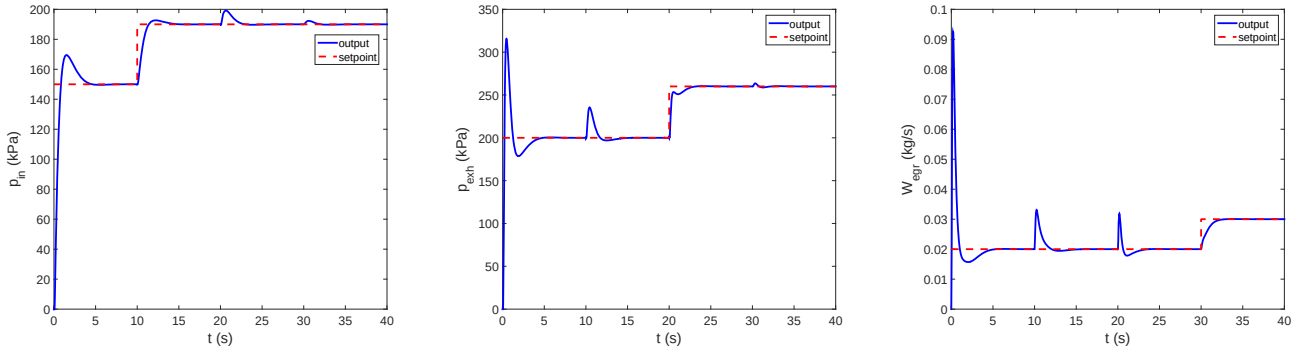

(a) p_{in} tracking (b) p_{exh} tracking (c) W_{egr} tracking

Fig. 8. Tracking performance evaluation in simulation

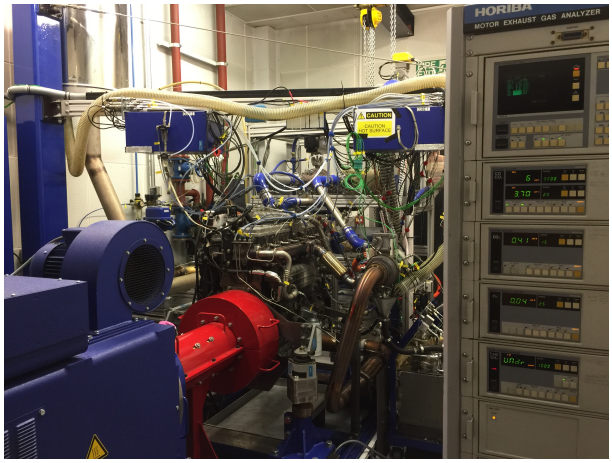

Fig. 9. ETA-fitted heavy-duty engine experimental platform

torque of 1280 Nm at 1400 rpm. The engine is fitted with an ETA and a high pressure loop cooled EGR. The ETA was developed by a consortium led by Caterpillar. Based on the ETA, several control methods and testing systems were developed in Loughborough University in simulations [23]–[25] and experiments [26].

The tracking performance of the proposed 3-input 3-output (3I3O) controller at 1800 rpm, 260 Nm is illustrated in Fig. 10. At the initial stage, step changes are set on p_{in}^* between 30 kPa and 60 kPa, while the other setpoints are kept as constants. The control laws are changing fast to respond the change on p_{in}^*. When p_{in}^* drops from 60 kPa to 30 kPa, χ_{vgt} increases immediately, while P_{em} is pushed from motoring mode into generating mode. At the same time, χ_{egr} reduces slightly. The actuators work together to achieve a low p_{in}. When W_{egr}^* changes from 100 kg/h to around 0 kg/h at about 180 s, χ_{egr} is forced to shut off. Meanwhile, closing χ_{vgt} and increasing P_{em} both guarantee the steady value of p_{in} and p_{exh}. When p_{exh}^* drops from 95 kPa to 80 kPa at 360 s, the controller reduces χ_{vgt} and increases χ_{egr} to achieve lower p_{exh}. In additional, P_{em} is increased to maintain p_{in}. The tracking performance is desirable with variable setpoints on control variables.

VI. Conclusions

A model-based MIMO robust decoupling controller of a newly designed ETDE is given in this paper. Stability margins are considered in building the controller and therefore, strong robustness is held. The proposed controller showed excellent tracking performance in both transients and steady states and is applicable in industrial applications. Experimental results strongly support the effectiveness of the the proposed controller. This work effectively underpin the next stage real-time optimization on fuel economy of ETDE.

Acknowledgement

This work was co-funded by the Innovate UK, under a grant for the Low Carbon Vehicle IDP4 Programme (TP14/LCV/6/I/BG011L). The Innovate UK is an executive body established by the United Kingdom Government to drive innovation. It promotes and invests in research, development and the exploitation of science, technology and new ideas for the benefit of business - increasing sustainable economic growth in the UK and improving quality of life.

References

[1] (2015, Dec.) Adoption of the paris agreement. United Nations. Paris, France. [Online]. Available: https://unfccc.int/resource/docs/2015/cop21/eng/l09.pdf

[2] (2012, Nov.) Global transportation energy and climate roadmap: The impact of transportation policies and their potential to reduce oil consumption and greenhouse gas emissions. The International Council on Clean Transportation. Washington DC, United States. [Online]. Available: http://www.theicct.org/sites/default/files/publications/ICCT%20Roadmap%20Energy%20Report.pdf

[3] A. Bin Mamat, R. Martinez-Botas, S. Rajoo, A. Romagnoli, and S. Petrovic, "Waste heat recovery using a novel high performance low pressure turbine for electric turbocompounding in downsized gasoline engines: Experimental and computational analysis," *Energy*, vol. 90, no. 1, pp. 218–234, 2015.

[4] H. Tang, A. Pennycott, S. Akehurst, and C. J. Brace, "A review of the application of variable geometry turbines to the downsized gasoline engine," *International Journal of Engine Research*, vol. 16, no. 6, pp. 810–825, 2015.

[5] H. Tang, A. Pennycott, S. Akehurst, and C. J. Brace, "Effects of exhaust gas recycle in a downsized gasoline engine," *Applied Energy*, vol. 105, pp. 99–107, May 2013.

[6] P. Divekar, B. Ayalew, and R. Prucka, "Coordinated electric supercharging and turbo-generation for a diesel engine," *SAE International*, pp. 2010–01–1228, 2010.

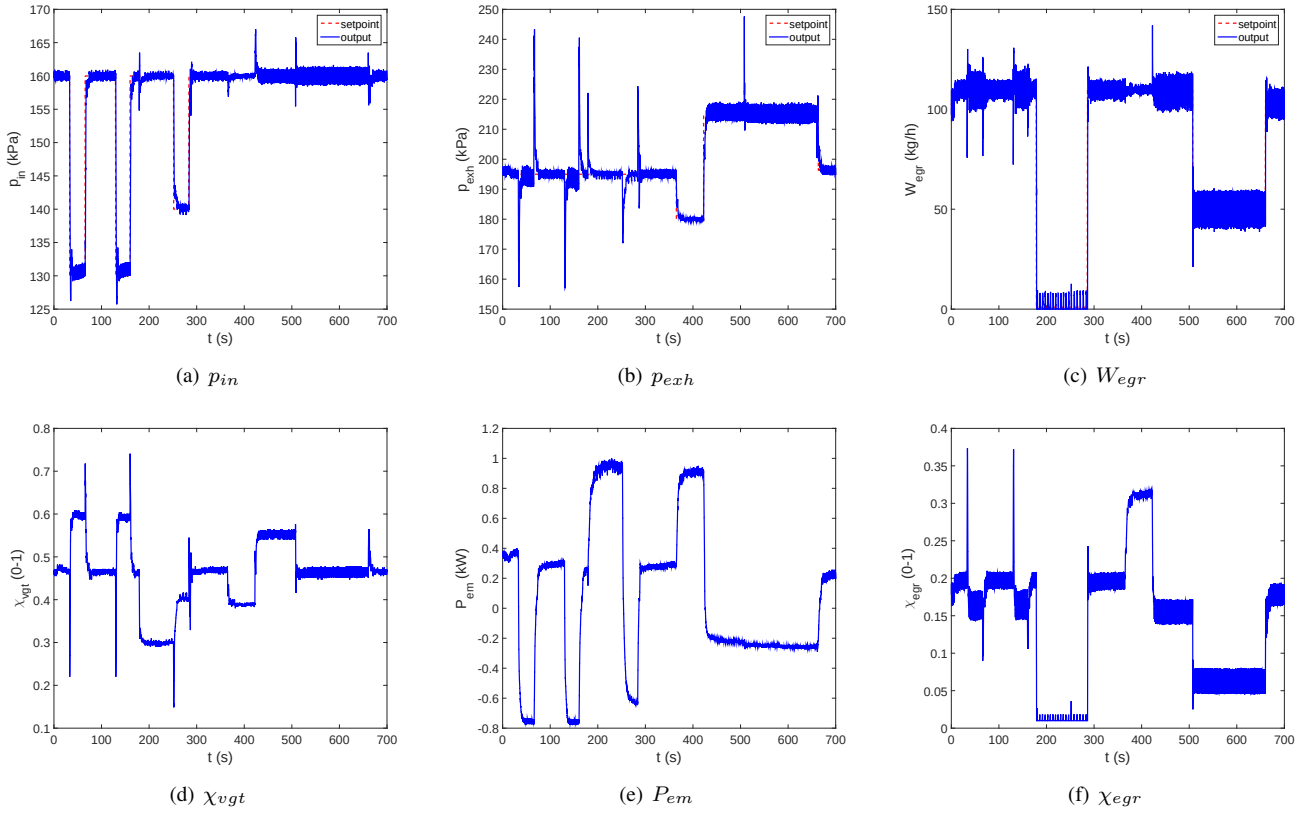

(a) p_{in} (b) p_{exh} (c) W_{egr}

(d) χ_{vgt} (e) P_{em} (f) χ_{egr}

Fig. 10. Tracking performance of the 3I3O robust controller with variable setpoints at 1800rpm, 260Nm

[7] L. Eriksson, T. Lindell, O. Leufven, and A. Thomasson, "Scalable component-based modeling for optimizing engines with supercharging, e-boost and turbocompound concepts," *SAE International Journal of Engines*, pp. 2012–01–0713, 2012.

[8] M. Bailey, "Electrically-assisted turbocharger development for performance and emissions," in *Proceedings of the Diesel Engine Emissions Reduction Workshop*, 2000, p. 827803.

[9] S. Arnold, C. Balis, P. Barthelet, E. Poix, T. Samad, G. Hampson, and S. Shahed, "Garrett electric boosting systems (EBS) program," Honeywell Turbo Technologies, Rolle, Switzerland, Tech. Rep. DE-FC05-00OR22809, June 2005.

[10] S. Ibaraki, Y. Yamashita, K. Sumida, H. Ogita, and Y. Jinnai, "Development of the hybrid turbo, an electrically assisted turbocharger," *Mitsubishi Heavy Industries Technical Review*, vol. 43, no. 3, pp. 1–5, 2006.

[11] (2012) Generating insight, edition 2. Cummins Generator Technologies. Peterborough, United Kingdom. [Online]. Available: http://stamford-avk.com/media/generating-insight-magazine

[12] N. Terdich, R. Martinez-Botas, D. Howey, and C. Copeland, "Off-road diesel engine transient response improvement by electrically assisted turbocharging," *SAE International*, pp. 2011–24–0127, 2011.

[13] N. Terdich and R. Martinez-Botas, "Experimental efficiency characterization of an electrically assisted turbocharger," *SAE International*, pp. 2013–24–0122, 2013.

[14] N. Terdich, R. Martinez-Botas, A. Romagnoli, and A. Pesiridis, "Mild hybridization via electrification of the air system: Electrically assisted and variable geometry turbocharging impact on an off-road diesel engine," *Journal of Engineering for Gas Turbines and Power-Transactions of the ASME*, vol. 136, no. 3, p. 031703, 2014.

[15] A. Costall, R. Ivanov, and T. Langley, "Electric turbo assist as an enabler for engine downspeeding," in *Proceedings of the ASME Turbo Expo*, 2012, pp. 511–521.

[16] A. Costall, R. Ivanov, and T. Langley, "Electric turbo assist: efficient rapid boost for heavy duty diesel engines," in *Proceedings of the Conference on Thermo and Fluid Dynamic Processes in Direct Injection Engines*, 2012, pp. 1–18.

[17] S. Larguech, S. Aloui, O. Pages, A. Hajjaji, and A. Chaari, "Fuzzy sliding mode control for turbocharged diesel engine," *Journal of Dynamic Systems, Measurement, and Control*, vol. 138, p. 011009, 2016.

[18] S. Katayama, K. Yubai, and J. Hirai, "Iterative design of the reduced-order weight and controller for the H_∞ loop-shaping method under open-loop magnitude constraints for siso systems," *IEEE Transactions on Industrial Electronics*, vol. 56, no. 10, pp. 3854–3863, 2009.

[19] K. Tsakalis, S. Dash, A. Green, and W. MacArther, "Loop-shaping controller design from input-output data: application to a paper machine simulator," *IEEE Transactions on Control Systems Technology*, vol. 10, no. 1, pp. 127–136, 2002.

[20] A. Genc, "A state-space algorithm for designing H_∞ loop shaping pid controllers," University of Cambridge, Cambridge, U.K., Tech. Rep. DEC-TR-506, October 2000.

[21] T. Lee, S. Chiang, and J. Chang, "H_∞ loop-shaping controller designs for the single-phase UPS inverters," *IEEE Transactions on Power Electronics*, vol. 16, no. 4, pp. 473–481, 2001.

[22] D. McFarlane and K. Glover, "A loop shaping design procedure using H_∞ synthesis," *IEEE Transactions on Automatic Control*, vol. 37, no. 6, pp. 759–769, 1992.

[23] D. Zhao and R. Stobart, "Systematic control on energy recovery of electrified turbocharged diesel engines," in *Proceedings of the 54th IEEE Conference on Decision and Control*, 2015, pp. 1527–1532.

[24] D. Zhao, E. Winard, Z. Yang, R. Stobart, and T. Steffen, "Decoupling control of electrified turbocharged diesel engines," in *Proceedings of the American Control Conference*, 2016, pp. 4207–4212.

[25] D. Zhao, E. Winard, Z. Yang, R. Stobart, and T. Steffen, "Real-time optimal energy management of electrified engines," in *Proceedings of the 8th IFAC Symposium on Advances in Automotive Control*, June 2016, pp. 251–258.

[26] E. Winward, J. Rutledge, J. Carter, A. Costall, R. Stobart, D. Zhao, and Z. Yang, "Performance testing of an electrically assisted turbocharger on a heavy duty diesel engine," in *Proceedings of the 12th International Conference on Turbochargers and Turbocharging*, 2016.